

## PARAGON2 Depletion Validation Using SERPENT2 Monte Carlo Code<sup>1</sup>

Mohamed Ouisloumen

Fuel Engineering, Westinghouse Electric Company LLC, Cranberry Twp, Pennsylvania, USA  
ouislom@westinghouse.com

**Abstract** - This paper presents a thorough comparison of PARAGON2 against the continuous energy Monte Carlo code SERPENT2. The objective of this paper is to demonstrate that the new Westinghouse lattice physics code, PARAGON2, can reproduce the continuous energy Monte Carlo solution with the desired accuracy. A variety of PWR assembly test cases were selected to carry out this validation. These assemblies were modeled in both codes in various operating reactor core conditions including the depletion. Excellent agreements between PARAGON2 and SERPENT2 were obtained for reactivity and pin power parameters, in all conditions and throughout the depletion.

### I. INTRODUCTION

PARAGON2 is the new Westinghouse lattice physics code that is under validation and qualification. PARAGON2 [1] departs from the traditional lattice codes by using very fine energy mesh for multi-group cross section calculations and incorporating numerous other enhancements; including, more detailed isotopic depletion chains.

In several instances, PARAGON2 was compared to Monte Carlo solution, but only, for snapshot steady state calculations. The emerging SERPENT2 [2] code has several attractive capabilities that make it a suitable Monte Carlo reference solution. Amongst these capabilities the depletion feature in SERPENT2 uses a more robust depletion solver based on Chebyshev Rational Approximation Method (CRAM) [3]. SERPENT2 has also implemented the resonance scattering model (RSM) which makes it comparable to PARAGON2.

The depletion modules in the industrial lattice physics codes are, usually, based on simplified theoretical models to minimize the computational running time. PARAGON2 is not an exception to this rule. The transmutation system of equations in PARAGON2 burnup calculation module uses the linearization of the depletion chains and the Laplace transform method for solution. As a consequence, complex depletion chains are replaced by simplified ones. For example, the cyclic transmutations occurring for the actinides appearing at high burnups are not explicitly modeled. The CRAM approach does not suffer from these limitations which makes SERPENT2 a relevant reference solution.

Benchmarking the industrial lattice codes against high order methods - usually continuous energy Monte Carlo - is one of the prerequisites to achieve the qualification of these codes for core design applications. In essence, we will compare PARAGON2 and SERPENT2 depletion results for various Westinghouse and Combustion Engineering (CE) PWR fuel assembly types (from 14×14 to 17×17, different enrichments, different burnable absorbers, etc). The comparison will also include different operating plant conditions such as fuel temperatures, moderator density, fuel contents, etc. The accident tolerant fuel was also included in the evaluation as the next generation of the fuel assembly product.

This paper is organized as follows: the next section

will give an overview of the new models implemented in PARAGON2. The assemblies selected for benchmarking are described in Section III. Section IV is reserved for the results and analyses. The concluding remarks are given in Section V.

### II. OVERVIEW OF PARAGON2 LATTICE CODE

The development of PARAGON2 is founded on first principle physics models; which, permits the avoidance of weak approximations in the solution algorithms of the transport equation. The objective is to come up with a state of the art lattice physics code that can improve the predictions in current operating plants, and at the same time produce a code capable of modeling the next generation of fuel products that are currently in research phase, such as the accident tolerant fuel. With this strategy, it becomes possible to develop a code that can be used for any type of fuel assembly regardless of the complexities of its geometry design and compositions.

The advanced methods used in PARAGON2 are computationally intensive. To offset this inconvenience, parallel computing algorithms were introduced throughout the code using the shared-memory multi-core processing OpenMP directives. The shared-memory approach is suitable for the kind of applications that PARAGON2 will be used for in core design analysis. With a modest computing power, one can easily achieve the required running time for few-group cross-sections generations, used in core simulators.

The main new improvements incorporated in PARAGON2 are summarized as follows:

- PARAGON2 uses the ultra-fine energy mesh cross-sections library with 6064 energy groups. The library will eventually contain all the isotopes available in ENDF/B7.1 basic nuclear data repository. This new library has been extensively benchmarked against Monte Carlo continuous energy solution for all types of fuel assemblies, currently in use, and against critical experiments. It is important to note that the cross-sections of this library are processed through NJOY [4] code and are used, as they are, from the source without any adjustment.
- All the scattering matrices of the isotopes in UFEML are based on the anisotropic resonance scattering model described in Ref. [5], except for hydrogen in water and

<sup>1</sup>© 2017 Westinghouse Electric Company LLC. All Rights Reserved.

the graphite as addressed in Ref. [5].

- The depletion chains in PARAGON2 have been extended to track 116 fission products and 25 actinides. In the point of view of the memory management and the running time performance of the code, these detailed depletion chains are a challenging problem for UFEML method. The energy dependent fission products yields were also implemented in PARAGON2, if available within ENDF/B7.1.
- All the modules in the code that necessitate the multi-group energy formulation use the 6064 groups without any collapse inside the code. This approach requires sophisticated programming algorithms for better memory management.

The collision probability and interface current methods were used in the flux solution as described in Ref. [5].

### III. ASSEMBLY TEST CASES

#### 1. 14×14 Fuel Assembly Type with IFBA and Gadolinium

This assembly is a new 14×14 fuel design that has both IFBA (Integral Fuel Burnable Absorber) and gadolinium burnable absorbers in the same assembly configuration. This fuel will be deployed in one of the domestic plants in the near future. The assembly considered for this benchmarking has the following characteristics:

- 112 IFBA (1.5×) rods with a fuel enrichment of 4.87 w/o
- 8 rods with uranium enrichment of 2.92 w/o and gadolinium enrichment of 8 w/o .
- The remaining 59 fuel rods have the same enrichment as IFBA rods
- The assembly has 16 guide tubes and one instrumentation thimble rod.

The cell pitch is 1.414488 cm, the fuel rod diameter is 0.935852 cm, and the other dimensions are typical for 14×14 fuel type. PARAGON2 calculations were carried out using four sub-regions in the fuel pellet with volumes corresponding to 50%, 25%, 15% and, 10% of the total pellet volume. The current coupling order was set to seven. The moderator region is subdivided azimuthally into four sub-regions. The SERPENT2 model uses ten equal volume rings per pellet to better predict the fuel isotopic radial distribution within the pellet (especially the plutonium distribution) during the depletion. It is important to mention that the usage of four regions in PARAGON2 modeling is equivalent to ten rings (i.e. reproduces the ten rings results), and it is consistent with the model used in core design calculations.

The depletion of this assembly was done using the asymptotic and resonance scattering models. The temperatures with the asymptotic scattering are 900°K for fuel regions and 600°K for other cell regions (cladding and moderator). For the resonance scattering, the temperature for the fuel regions was set to 1500°K. We selected this temperature to emphasize the effect of the resonance scattering model and consequently highlight

any discrepancy that may exist between two codes. The predictor/corrector methodology was enabled in both codes. The same set of 89 burnup depletion steps was also used in both runs. The burnup delta steps used are 250 MWD/MTU at the beginning of depletion, 500 MWD/MTU at the middle, and 1000 MWD/MTU at the end. The moderator boron content was kept constant during the depletion with a value of 981 ppm.

The SERPENT2 calculation scheme consists of using 500000 neutron histories per cycle for a total of 200 active cycles. In order to better converge the neutron source distribution, 100 inactive cycles were used. All boundary conditions were set to be reflective in both code models. This fuel assembly case is particularly challenging because of the strong heterogeneity of its design induced by the presence of two strong burnable absorbers. The large cell pitch and the fuel rod diameter also contribute to the complexity of the modeling.

#### 2. 15×15 Fuel Assembly Type with IFBA and WABA

This assembly corresponds to a typical 15×15 fuel design encompassing IFBA and WABA (Wet Annular Burnable Absorber) burnable poisons. This fuel type is currently loaded in some domestic plants. It has 148 fuel rods with IFBA, 16 WABA rods, 4 guide tubes, 1 instrumentation thimble, and the remaining 56 cells are filled with standard fuel rods. The enrichment of the fuel in all locations is 4.95 w/o. The cell pitch is 1.432322 cm, the fuel rod diameter is 0.93512 cm, and the other dimensions are typical for 15×15 fuel type. The WABA rods are modeled explicitly, without smearing any region. For both PARAGON2 and SERPENT2, the same detailed modeling used in the 14×14 case is also employed in this case. This includes the pellet splitting and depletion options. However, the boron concentration used in this case is 500 ppm.

#### 3. Westinghouse 16×16 Fuel Assembly Type with Gadolinium

The 16×16 Westinghouse design fuel assembly was considered in this case, but with gadolinium as burnable absorber. The cell pitch is the typical 16×16 value of 1.233970 cm. However, the fuel rod diameter is slightly smaller with a value of 0.789572 cm. The uranium enrichment is 4.8 w/o for normal pellets. The enrichments for gadolinia rods are 3.36 w/o and 6 w/o for uranium and gadolinium, respectively. This assembly contains 16 gadolinia rods, 20 guide tubes, 1 instrumentation thimble, and the remaining 219 rods are normal fuel rods. In both PARAGON2 and SERPENT2 runs:

- The gadolinium pellets were modeled with ten equal volume rings.
- The same other 14×14 cells representations are used here.
- The boron concentration in these models is set to 1830 ppm.

#### 4. Westinghouse 16×16 Fuel Assembly Type with IFBA

In this test case, the typical 16×16 Westinghouse design assembly is considered. This assembly contains 116 IFBA

fuel rods, 119 normal fuel rods, 20 guide tubes, and 1 instrumentation thimble. The enrichments of both fuel rod types is 4.95 w/o. The cell pitch is 1.236863 cm, the fuel pellet diameter has the standard value of 0.823734 cm. Other dimensions are the regular 16×16 types. PARAGON2 simulations in this case used ten equal volume rings. The boron concentration in the moderator is 500 ppm. The other options used in SERPENT2 and in PARAGON2 calculations are the same as in the 14×14 case.

### 5. CE 16×16 Fuel Assembly Type with IFBA

The Combustion Engineering (CE) 16×16 assembly design was selected for this case. It has four 2×2 large guide tubes, one 2×2 instrumentation thimble, and the remaining locations are filled with fuel cells. This assembly has an enrichment zoning with:

- 92 IFBA rods with uranium enrichment of 4.56 w/o,
- 44 IFBA rods with 4.16 w/o uranium enrichment,
- 92 normal fuel rods with an enrichment of 4.56 w/o,
- 8 regular fuel rods with 4.16 w/o enrichment.

The cell pitch is 1.287336 cm, the fuel pellet diameter is 0.824528 cm, and the others design dimensions are the typical CE 16×16 assembly type. PARAGON2 models employed ten equal volume rings for all fuel pellets. The boron concentration in the moderator is 712 ppm. The other options used in SERPENT2 and in PARAGON2 calculations are the same as in the 14×14 case.

### 6. CE 16×16 Fuel Assembly Type with ATF

The Accident Tolerant Fuel (ATF) is a new fuel concept currently in research stage. The purpose of this task is to confirm the PARAGON2 ability to accurately model this kind of fuel. The CE assembly selected is similar to the previous case. The fuel material used here is  $U_3Si_2$ , with one single enrichment of 5.0 w/o. The cell pitch is 1.2850 cm and the pellet diameter is 0.82677 cm. The same modeling options used in the previous case are also adopted for this case. Approximately, 748 ppm of boron is used in the calculations.

From neutronics point of view, this case is interesting because of its high fuel density and its representation of the next generation of fuel product.

### 7. 17×17 Fuel Assembly Type with IFBA and WABA

This case is the typical Westinghouse 17×17 standard fuel design used in the reactor core described in Reference [6]. It features radial enrichment zoning with an average enrichment of 3.8 w/o  $^{235}U$  (enrichments used are 3.4 w/o, 3.8 w/o, and 4.2 w/o). This case has 68 rods with pellets coated with IFBA and 12 WABA discrete burnable inserts. Design details of this case are available in Ref. [6]. The cell representation modeling used for both codes is identical to the case of 14×14. This includes the mesh discretization and depletion options. Throughout the depletion, a constant 500 ppm of boron is used.

### 8. MOX Fuel Assembly

The pins layout in this case is a standard 17×17 fuel type. Three types of fuel pellets are used, corresponding to three Plutonium fissile enrichments of 4.95 w/o, 3.19 w/o, and 1.80 w/o. This fuel design is a typical MOX fuel assembly, currently loaded in European plants. The cell pitch between the fuel rods is 1.262085 cm and the pellet diameter is 0.823508 cm. The other dimensions are equivalent to the 17×17 Westinghouse design. The boron concentration used is 500 ppm. It is kept constant during the depletion. PARAGON2 models used ten equal volume rings for all pellets. As in the case of 14×14, the same other modeling options are used for both SERPENT2 and PARAGON2 runs.

## IV. RESULTS AND ANALYSES

### 1. Comparison of CZP, HZP, and HFP BOL Results

In Table I, PARAGON2 is compared to SERPENT2 for all the assembly cases defined in Section III. The comparison was first made for the cold zero power (CZP) conditions, where the temperature was set to 300°K for all regions in the assemblies. The results obtained were very good. Indeed, the absolute maximum difference between two codes is  $\leq 80$  pcm for all cases with an average of  $\sim -40$  pcm (which is within 95% confidence interval (CI) of SERPENT2 results).

The next run was done for Hot Zero Power (HZP) condition where the isothermal temperature used is 600°K. The results obtained were, again, very good and slightly better than the cold case, with an average of  $-23$  pcm (within 95% CI of SERPENT2 statistics). The maximum absolute difference is also slightly better with a value of 65 pcm.

The Hot Full Power (HFP) results are also displayed in Table I for zero burnup. Two calculations with and without control rods inserted were carried out. The fuel temperature in these cases is 900°K, while the temperature of the other assembly regions (clad, moderator, etc) is set to 600°K. The control rod material used for all cases is made of silver (Ag), Indium (In), and Cadmium (Cd). The results for this HFP cases are excellent. The maximum absolute difference is 68 pcm and 48 pcm for rodDED and unrodDED cases, respectively, with an average of  $\sim 7$  pcm for rodDED runs and  $\sim -6$  pcm for unrodDED assemblies (which are within  $1\sigma$  deviation of SERPENT2 statistical results).

The results obtained in this section show that PARAGON2 can reproduce the Monte Carlo continuous results for CZP, HZP and HFP conditions. The rod worth predicted by PARAGON2 is also very close to Monte Carlo continuous energy results for all fuel types. A closer look to the results shows that there is a slight trend with low temperature and hard spectrum. In these situations, the resonance range plays a bigger role. This suggests that, for some extreme situation, there may be some resonances that are not well described by the energy mesh used in UFEML. This mesh may be improved in the future; however, this will have negligible impact in the core design analyses.

Note that, in Table I, 14×14 case correspond to the assembly described in Section III.1, 15×15 to the case in Section III.2,

W 16×16 Gad to the case in Section III.3, W 16×16 to the case in Section III.4, CE 16×16 to the case in Section III.5, CE 16×16 ATF to the case in Section III.6, 17×17 to the case in Section III.7, and MOX to the case in Section III.8.

Case	$k_{\infty}^{\text{PARAGON2}}$	$k_{\infty}^{\text{SERPENT2}}$	$\delta_k^{\text{Asymp}} (pcm)$
Cold Zero Power ( 300°K)			
14x14	1.02351	1.02419	-68
15x15	1.05297	1.05347	-50
17x17	1.09138	1.09194	-56
W 16x16 Gad	1.10597	1.10669	-72
CE 16x16 ATF	1.37394	1.37388	6
W 16x16	1.17016	1.17095	-79
MOX	1.1591	1.15897	13
CE 16x16	1.02404	1.02415	-11
Hot Zero Power ( 600°K)			
14x14	1.00939	1.00988	-49
15x15	1.03906	1.03944	-38
17x17	1.07436	1.07391	45
W 16x16 Gad	1.08534	1.08558	-24
CE 16x16 ATF	1.36262	1.36291	-29
W 16x16	1.15631	1.15692	-61
MOX	1.14036	1.14101	-65
CE 16x16	1.01385	1.01346	39
Rodded - Hot Full Power ( Fuel 900°K, Others 600°K)			
14x14	0.78403	0.78390	13
15x15	0.8439	0.84396	-6
17x17	0.8615	0.86139	11
W 16x16 Gad	0.84734	0.84751	-17
CE 16x16 ATF	1.11492	1.11412	72
W 16x16	0.88365	0.88433	-68
MOX	0.90284	0.90294	-10
CE 16x16	0.8503	0.84971	59
Hot Full Power ( Fuel 900°K, Others 600°K )			
14x14	1.00262	1.00288	-26
15x15	1.03222	1.03246	-24
17x17	1.13412	1.13380	32
W 16x16 Gad	1.07749	1.07776	-27
CE 16x16 ATF	1.35369	1.35356	13
W 16x16	1.14781	1.14832	-51
MOX	1.12939	1.12954	-15
CE 16x16	1.00714	1.00666	48

TABLE I. SERPENT2 Compared to PARAGON2 Using UFEML Asymptotic Cross-Section Library with  $\delta_k^{\text{Asymp}} = k_{\infty}^{\text{PARAGON2}} - k_{\infty}^{\text{SERPENT2}}$ . The SERPENT2  $1\sigma$  standard deviation is  $\leq 15 pcm$  for all runs.

## 2. Comparison of the Depletion Results

### A. Reactivity Comparison

The assemblies described in Section III were depleted up to 70 GWD/MTU using SERPENT2 and PARAGON2. Figures 1 to 8 give the comparison of the reactivity as a function of burnup. The right y-axis of these figures gives the delta in

$pcm$  between PARAGON2 and SERPENT2 as  $\delta_k = k_{\infty}^{\text{P2}} - k_{\infty}^{\text{S}}$ , where  $k_{\infty}^{\text{P2}}$  and  $k_{\infty}^{\text{S}}$  are the neutron multiplication factors (eigenvalues) of PARAGON2 and SERPENT2. Two delta values are plotted in each figure. The first one (black lines, marked as  $\delta^{\text{Asymp}}$ ) corresponds to the comparison performed using the asymptotic elastic neutron scattering model. The second comparison (red lines, marked as  $\delta^{\text{RSM}}$ ) corresponds to the cases with the resonance scattering model turned on in both codes. The figures contain also the plots of both SERPENT2 and PARAGON2 eigenvalues ( $k_{\infty}^{\text{S}}$  and  $k_{\infty}^{\text{P2}}$  in the left y-axis) for the results with the asymptotic scattering model (the RSM results have the same behavior and are not included in the figures).

All the isotopes in PARAGON2 cross section library employ the resonance scattering model. For SERPENT2, only the following isotopes had this option turned on:  $^{235}\text{U}$ ,  $^{238}\text{U}$ ,  $^{238}\text{Pu}$ ,  $^{239}\text{Pu}$ ,  $^{240}\text{Pu}$ ,  $^{241}\text{Pu}$ ,  $^{242}\text{Pu}$ ,  $^{244}\text{Cm}$ ,  $^{90}\text{Zr}$ , and  $^{91}\text{Zr}$ . The intent was to have the resonance scattering effect accounted for uranium and plutonium isotopes, for neutron energies between 0.1 eV and 300 eV.

Table II summarizes the results in Figures 1 to 8. This table presents the average (Avg), the standard deviation (StDev), the maximum, and the minimum of the differences for each case. For both the asymptotic and the RSM calculations, the average difference between SERPENT2 and PARAGON2 is  $\leq 75 pcm$  with a maximum standard deviation of  $\sim 110 pcm$ . The maximum absolute difference obtained is  $\sim 230 pcm$ . Combining all the assembly cases, the statistics for the asymptotic runs are given in Fig. 9 for all the burnup points. Overall, the results in Fig. 9 are very good with an average difference of only  $-14 pcm$  with a standard deviation of  $79 pcm$ . The statistical two-sample t-test null hypothesis was also performed to compare PARAGON2 and SERPENT2 distributions (test of mean difference = 0). The P-value obtained is 0.981, indicating that there is not a statistically significant difference between the two results at the 95% confidence level. Therefore, this analysis confirms that PARAGON2 can reproduce the Monte Carlo continuous energy neutron multiplication factors with the desired accuracy  $\leq 200 pcm$ .

A closer look at the Figures 1 to 8 and to the Tables I and II show that:

- PARAGON2 and SERPENT2 agree very well at the beginning of cycle (zero burnup) and the differences between the two codes increase at the early stage of the depletion. These discrepancies diminish toward the middle and the end of the depletion. This is particularly evident for the assemblies with strong heterogeneities incited by the presence of burnable absorbers.
- The SERPENT2 values seem to fluctuate as a function of burnup. This is probably due to the “low number” of neutron histories used. However, these variations are within the statistical uncertainties.
- Table II shows larger and positive differences for the RSM averages (when compared to asymptotic results). This is probably due to the fact that PARAGON2 is using RSM for all isotopes, while only selected isotopes use

this model in SERPENT2. It may also be due to different implementations of the RSM theory in the codes.

Figure 9 shows that very few points are outside of the range of  $\pm 150$  pcm and only a couple of points above an absolute value of 200 pcm. This suggests that there are some minor differences in the way PARAGON2 and SERPENT2 perform the depletion. However, these differences are within the uncertainties that could arise from various numerical and physics models of the two codes. Therefore, the results obtained are indeed excellent and show that the depletion methods of PARAGON2 and SERPENT2 are equivalent without any apparent trend in the differences.

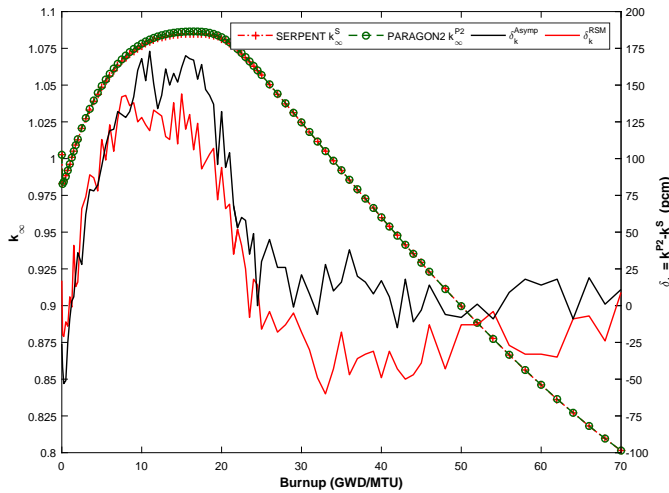


Fig. 1. Reactivity Comparison for  $14 \times 14$ . The left Y-axis shows the eigenvalues of the asymptotic models. The right Y-axis gives the differences between SERPENT2 and PARAGON2 for asymptotic ( $\delta_k^{Asymp}$ ) and RSM ( $\delta_k^{RSM}$ ) calculations.

### B. Pin Power Comparison

For each assembly described in Section III, the pin power distributions from PARAGON2 and SERPENT2 simulations are compared in Figures 10 to 17. Three burnup steps, that are 0 GWD/MTU, 10 GWD/MTU, and 70 GWD/MTU were selected for this comparison. The results in these figures are summarized in Table III. For all eight assemblies, the maximum absolute average of the differences between PARAGON2 and SERPENT2 for all burnups is  $\sim 0.02\%$ , with a maximum standard deviation of  $\sim 0.68\%$ . For the individual pins, the maximum absolute error obtained for all calculations is  $\sim 2.1\%$ . This maximum error occurred in the same case and burnup corresponding to the largest error on the eigenvalues, discussed previously. This is rather an isolated discrepancy as it can be seen in the overall statistics given in Fig. 18, where the mean of the differences is  $\sim 0.0\%$ , with a standard deviation of  $\sim 0.4\%$ . As the burnup increases, the difference between the codes decreases (probably because the power tends to be smooth at high burnups). The examination of the results in these tables and figures do not show any trend as a function of any assembly characteristics such as geometry or

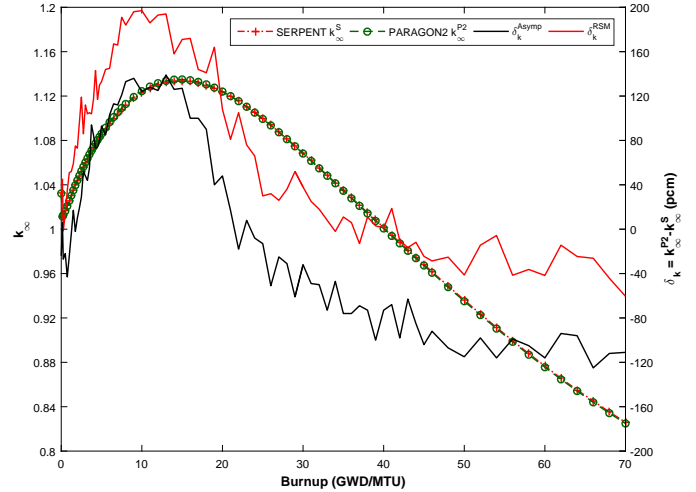


Fig. 2. Reactivity Comparison for  $15 \times 15$ . The left Y-axis shows the eigenvalues of the asymptotic models. The right Y-axis gives the differences between SERPENT2 and PARAGON2 for asymptotic ( $\delta_k^{Asymp}$ ) and RSM ( $\delta_k^{RSM}$ ) calculations.

materials configurations. However, slightly larger discrepancies are obtained for strongly heterogeneous fresh assemblies, but these differences are within the expected deviations. The predictions of PARAGON2 are remarkably very good and very consistent across all burnups and all fuel types.

### C. Comparison at High Void Conditions

The analyses considered so far are related to normal operating conditions in a PWR core. In this section, we want to compare PARAGON2 to SERPENT2 in conditions of loss of coolant accident. For this purpose, the  $16 \times 16$  with IFBA and the  $17 \times 17$  cases described in Sections III.4 and III.7 respectively were artificially modeled with 50% reduction of the moderator. The depletion is then performed in a manner similar to the previous analysis. Although this is an extreme situation for PWR cores, it represents a good benchmark for testing the lattice physics code to handle the accident scenarios. Figs. 19 and 20 display the differences between the eigenvalues of PARAGON2 and SERPENT2 as a function of burnup. At the beginning of the depletion, the differences between the codes are very similar to the normal cases; but as the assemblies get depleted this discrepancy grows. The reasons of these relatively larger differences are unknown. However, we suspect that the anisotropy scattering and other partial nuclear reactions ((n,Xn), inelastic, etc) models, that are affecting strongly these particular high void conditions, are not consistent between PARAGON2 and SERPENT2. The uncertainties sought in accident analyses simulations are far larger than the differences seen in Figs. 19 and 20. Therefore, PARAGON2 can still be applicable to analyze these abnormal situations. In future development, we will try to understand and correct these discrepancies.

Case	Asymptotic				RSM			
	Avg	StDev	Max	Min	Avg	StDev	Max	Min
14x14	62	67	173	-53	39	67	144	-60
15x15	-2	83	139	-125	64	75	197	-60
17x17	-55	37	32	-143	14	37	73	-53
W 16x16 Gad	2	52	146	-75	63	51	192	-28
CE 16x16 ATF	-36	30	19	-105	23	35	74	-46
W 16x16	-7	29	50	-81	65	27	114	-2
MOX	-71	91	56	-231	6	92	132	-138
CE 16x16	-7	111	157	-196	59	106	210	-142

TABLE II. Summary of the reactivity deltas for all burnup steps.

Case	0 GWD/MTU				10 GWD/MTU				70 GWD/MTU			
	Avg	StDev	Max	Min	Avg	StDev	Max	Min	Avg	StDev	Max	Min
14x14	0.00	0.45	1.21	-1.35	0.02	0.44	0.97	-1.26	0.00	0.31	0.71	-1.15
15x15	0.01	0.39	0.87	-0.78	0.00	0.21	0.47	-0.49	0.00	0.29	0.50	-0.85
17x17	0.00	0.33	0.73	-0.63	0.00	0.27	0.56	-0.71	0.00	0.36	0.56	-0.95
W 16x16 Gad	-0.01	0.46	1.80	-0.85	0.03	0.49	1.93	-1.19	0.00	0.37	1.15	-1.04
CE 16x16 ATF	0.01	0.43	0.82	-1.20	0.01	0.41	0.74	-1.16	0.00	0.32	0.78	-0.95
W 16x16	0.00	0.35	0.84	-1.25	0.00	0.39	0.72	-1.34	0.00	0.38	0.79	-1.30
MOX	-0.02	0.68	1.12	-2.10	-0.02	0.64	0.94	-1.77	0.00	0.34	0.74	-0.81
CE 16x16	-0.01	0.45	0.92	-0.92	0.03	0.38	0.62	-1.01	0.00	0.26	0.40	-0.71

TABLE III. Summary of the pin power deltas at burnups of 0 GWD/MTU, 10 GWD/MTU, and 70 GWD/MTU. The values are in relative percent:  $100 \times \frac{PARAGON2-SERPENT2}{PARAGON2}$

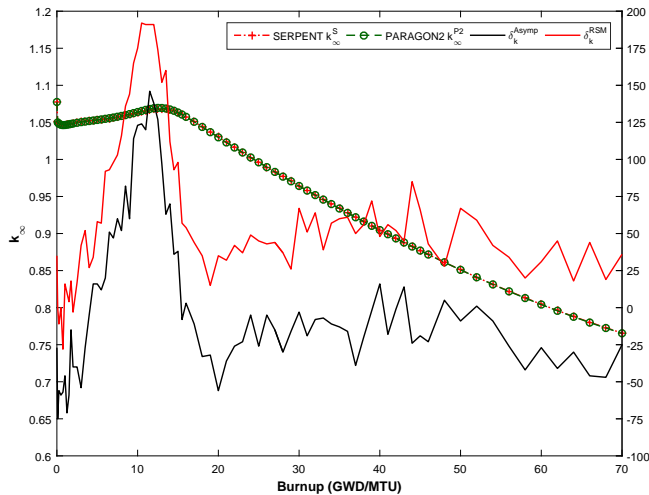


Fig. 3. Reactivity Comparison for Westinghouse 16x16 with gadolinium. The left Y-axis shows the eigenvalues of the asymptotic models. The right Y-axis gives the differences between SERPENT2 and PARAGON2 for asymptotic ( $\delta_k^{Asymp}$ ) and RSM ( $\delta_k^{RSM}$ ) calculations.

## V. CONCLUSIONS

In this paper, the SERPENT2 continuous energy Monte Carlo code was compared to PARAGON2. SERPENT2 has a more sophisticated depletion solution, while PARAGON2 uses simplified theory and depletion chains. Both codes have

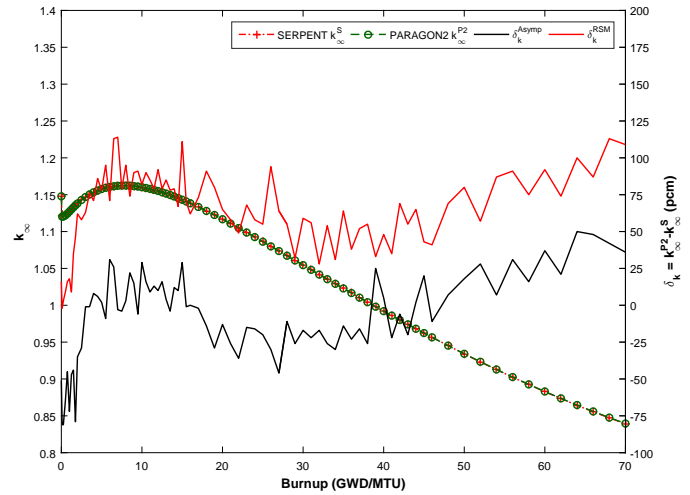


Fig. 4. Reactivity Comparison for Westinghouse 16x16 with IFBA. The left Y-axis shows the eigenvalues of the asymptotic models. The right Y-axis gives the differences between SERPENT2 and PARAGON2 for asymptotic ( $\delta_k^{Asymp}$ ) and RSM ( $\delta_k^{RSM}$ ) calculations.

implemented the resonance scattering theory.

Several PWR Westinghouse and CE design fuel assemblies were selected to perform the comparison. These cases cover all the Westinghouse fuel types currently in use or in development. All geometry types (from 14x14 to 17x17), enrichment range, and material compositions (UO<sub>2</sub>, MOX,

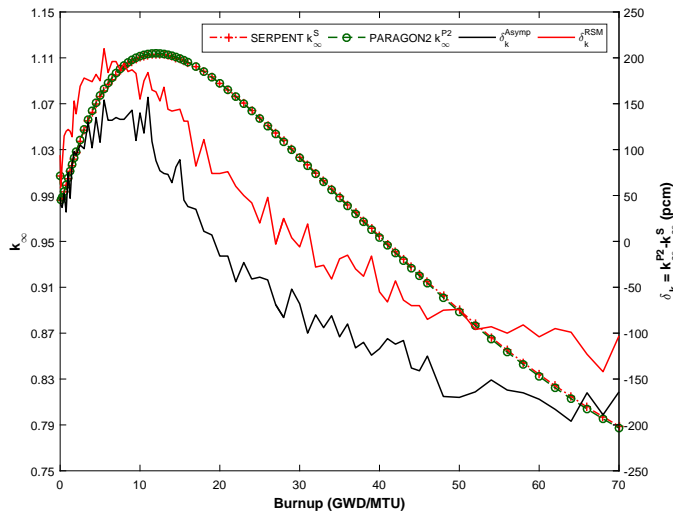


Fig. 5. Reactivity Comparison for CE 16×16 with IFBA. The left Y-axis shows the eigenvalues of the asymptotic models. The right Y-axis gives the differences between SERPENT2 and PARAGON2 for asymptotic ( $\delta_k^{Asymp}$ ) and RSM ( $\delta_k^{RSM}$ ) calculations.

IFBA, WABA, Gadolinium, etc) are considered. The selection was focused on choosing the most complex and challenging designs, such as the assemblies with the presence of IFBA and gadolinium burnable absorbers in the same configuration, the enrichments zoning, etc. The test cases were depleted using SERPENT2 and PARAGON2. The cross-section libraries of the two codes are also based on the same basic nuclear data of ENDF/B7.1.

The reactivity predictions (eigenvalues) of PARAGON2 and SERPENT2 were compared at CZP, HZP, and depleted HFP conditions. The control rod worth as well as the pin power distributions were also compared. The statistical analyses show that PARAGON2 is reproducing similar results as SERPENT2, and therefore, ascertains the adequacy of the PARAGON2 depletion module and the applicability of its fine energy mesh method for core design applications. Indeed, in average the eigenvalue differences are within  $\pm 100$  pcm and the maximum pin power differences are within  $\pm 2\%$ .

Although the results obtained for abnormal situations (i.e. high void) are acceptable, the analysis carried out in this paper indicates that improvements are needed in PARAGON2 to better predict these accident conditions. This will be the subject for the next development activities.

## VI. ACKNOWLEDGMENTS

The author is grateful to Jaakko Leppänen for providing SERPENT2 code and to Houda Ouisloumen for her help in editing this paper.

## REFERENCES

1. M. OUISLOUMEN, H. Q. LAM, and H. C. HURIA, “Predictions of PWR Cores Using PARAGON2 Based on Ultra-Fine Energy Mesh Cross-sections Libraries,” in “PHYSOR

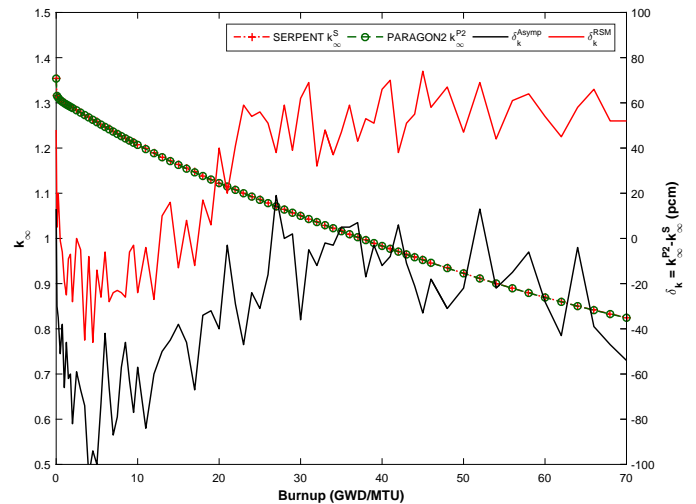


Fig. 6. Reactivity Comparison for CE 16×16 with ATF. The left Y-axis shows the eigenvalues of the asymptotic models. The right Y-axis gives the differences between SERPENT2 and PARAGON2 for asymptotic ( $\delta_k^{Asymp}$ ) and RSM ( $\delta_k^{RSM}$ ) calculations.

2016 - Unifying Theory and Experiments in the 21st Century,” Sun Valley Resort, Sun Valley, Idaho, USA (May 2016).

2. J. LEPPÄNEN, M. PUSA, T. VIITANEN, V. VALTAVIRTA, and T. KALTIAISENAHO, “The Serpent Monte Carlo code: Status, development and applications in 2013,” *Ann. Nucl. Energy*, **82**, 142–150 (August 2015).
3. M. PUSA, “Higher-Order Chebyshev Rational Approximation Method and Application to Burnup Equations,” *Nuclear Science and Engineering*, **182**, 3, 297–318 (MARCH 2016).
4. R. E. MACFARLANE and A. C. KAHLER, “Methods for Processing ENDF/B-VII with NJOY,” *Nuclear Data Sheets*, **111**, 2739 (2010).
5. M. OUISLOUMEN, A. M. OUGOUAG, and S. Z. GHAYEB, “Anisotropic Elastic Resonance Scattering Model for the Neutron Transport Equation,” *Nuclear Science & Engineering*, **179**, 59–84 (2015).
6. M. HONE, “AP1000 Core Reference Report,” WCAP 17524-NP, Westinghouse Electric Company LLC (March 2012).

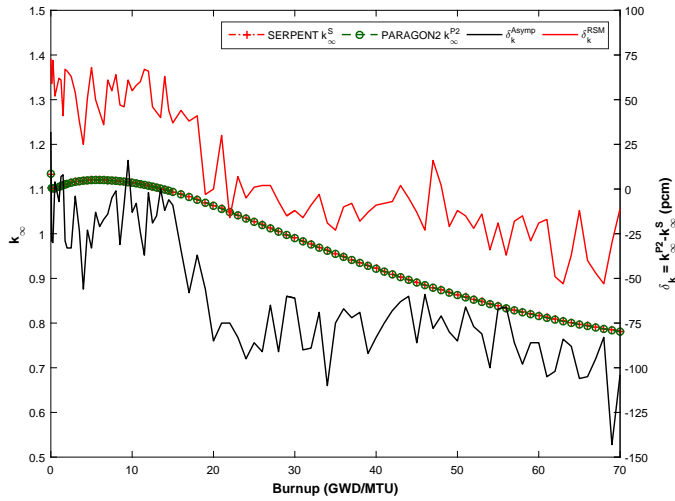


Fig. 7. Reactivity Comparison for  $17 \times 17$  with IFBA and WABA. The left Y-axis shows the eigenvalues of the asymptotic models. The right Y-axis gives the differences between SERPENT2 and PARAGON2 for asymptotic ( $\delta_k^{Asymp}$ ) and RSM ( $\delta_k^{RSM}$ ) calculations.

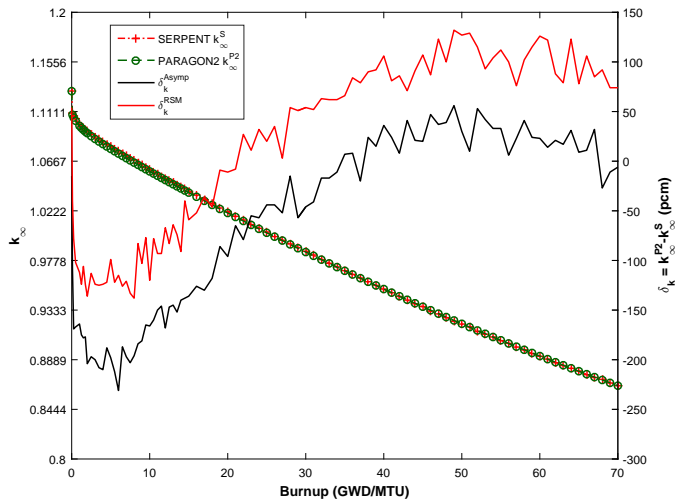


Fig. 8. Reactivity Comparison for zoned MOX  $17 \times 17$  assembly. The left Y-axis shows the eigenvalues of the asymptotic models. The right Y-axis gives the differences between SERPENT2 and PARAGON2 for asymptotic ( $\delta_k^{Asymp}$ ) and RSM ( $\delta_k^{RSM}$ ) calculations.

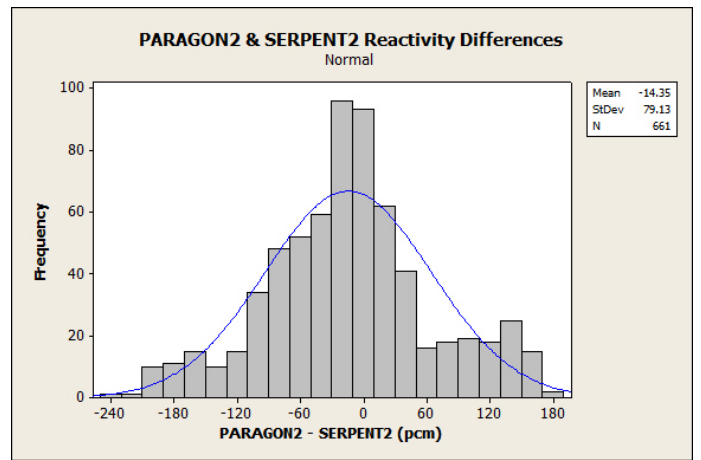


Fig. 9. Histogram of the reactivity ( $k_{\infty}$ ) differences.

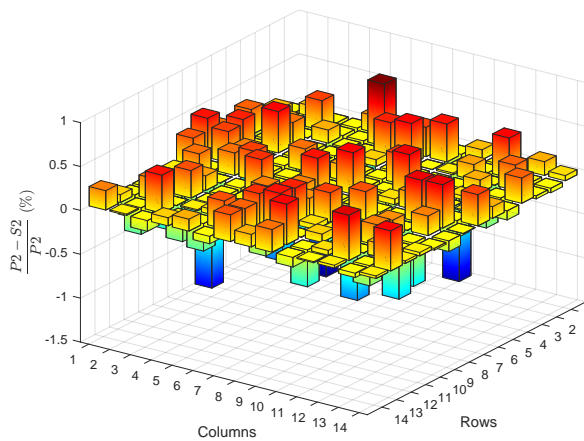
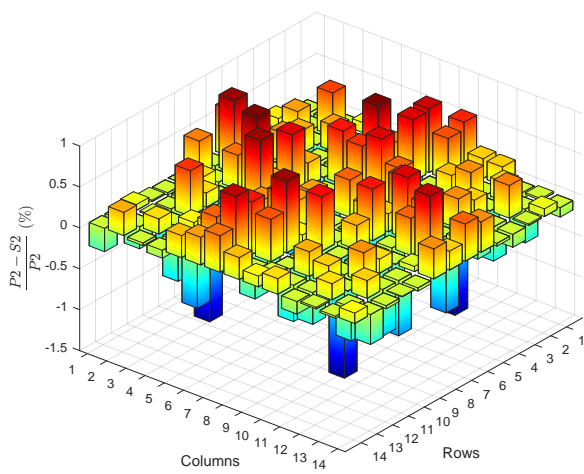
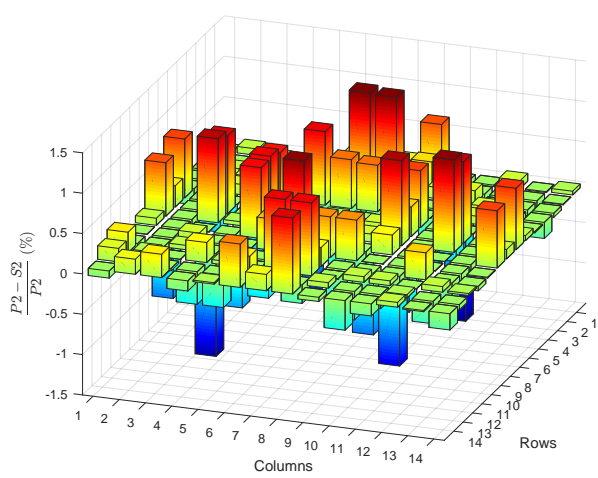


Fig. 10. Pin Power Comparison for 14x14 Assembly between PARAGON2 (P2) and SERPENT2 (S2). The top, middle, and bottom figures correspond to the burnups of 0, 10, and 70 GWD/MTU.

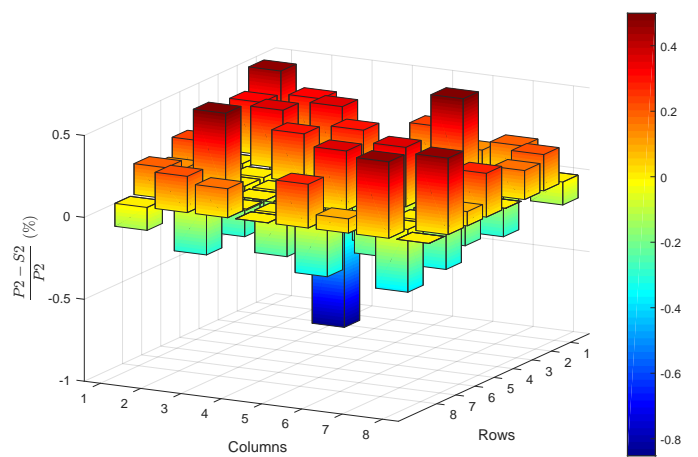
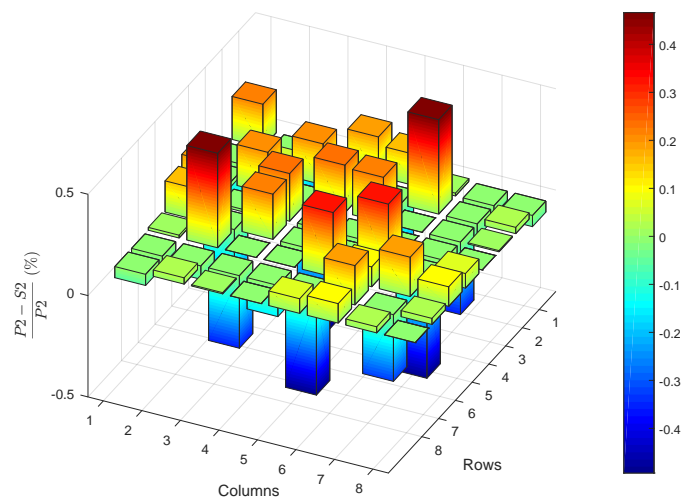
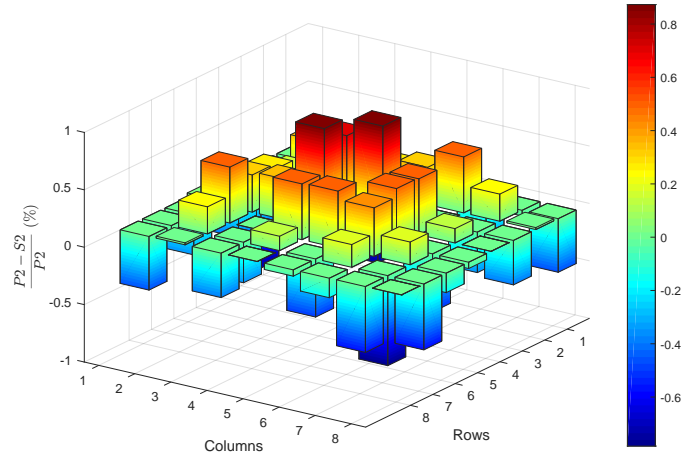


Fig. 11. Pin Power Comparison for 15x15 Assembly between PARAGON2 (P2) and SERPENT2 (S2). The top, middle, and bottom figures correspond to the burnups of 0, 10, and 70 GWD/MTU.

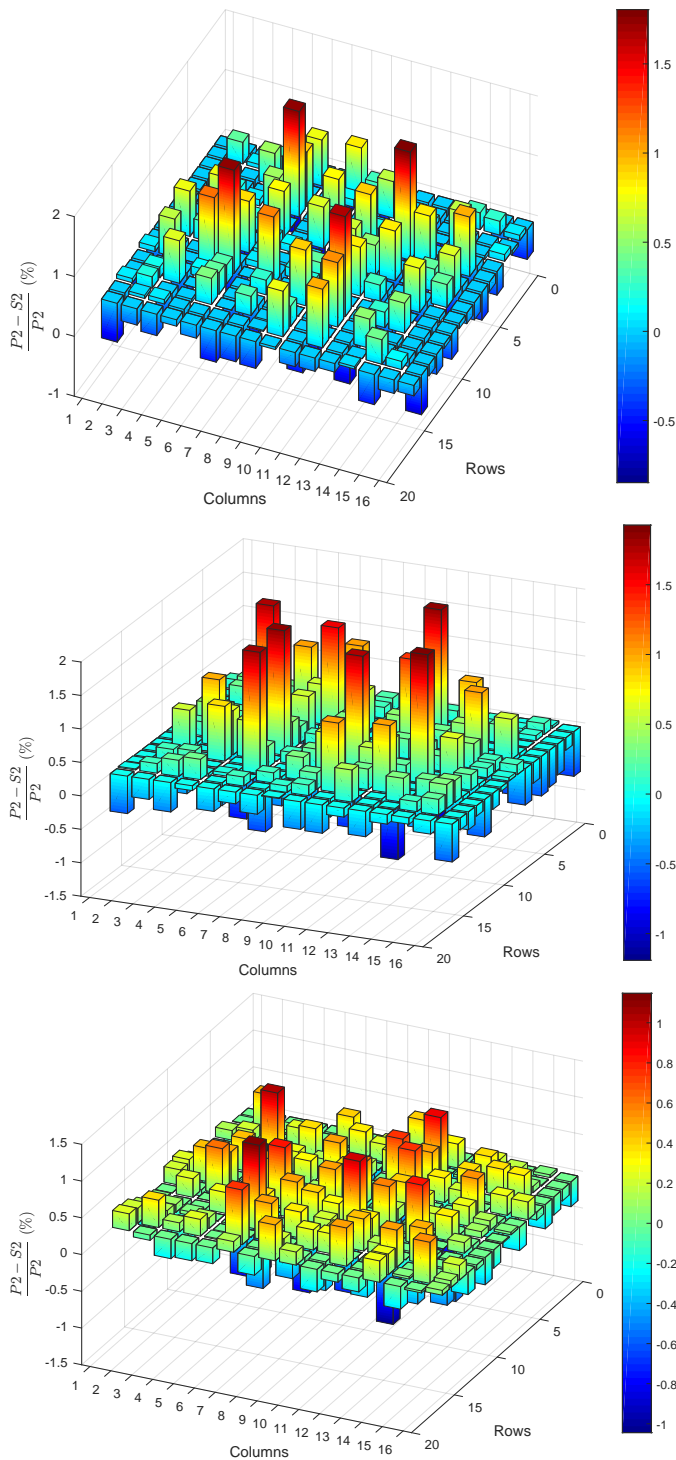


Fig. 12. Pin Power Comparison for Westinghouse 16x16 Assembly with Gadolinium between PARAGON2 (P2) and SERPENT2 (S2). The top, middle, and bottom figures correspond to the burnups of 0, 10, and 70 GWD/MTU.

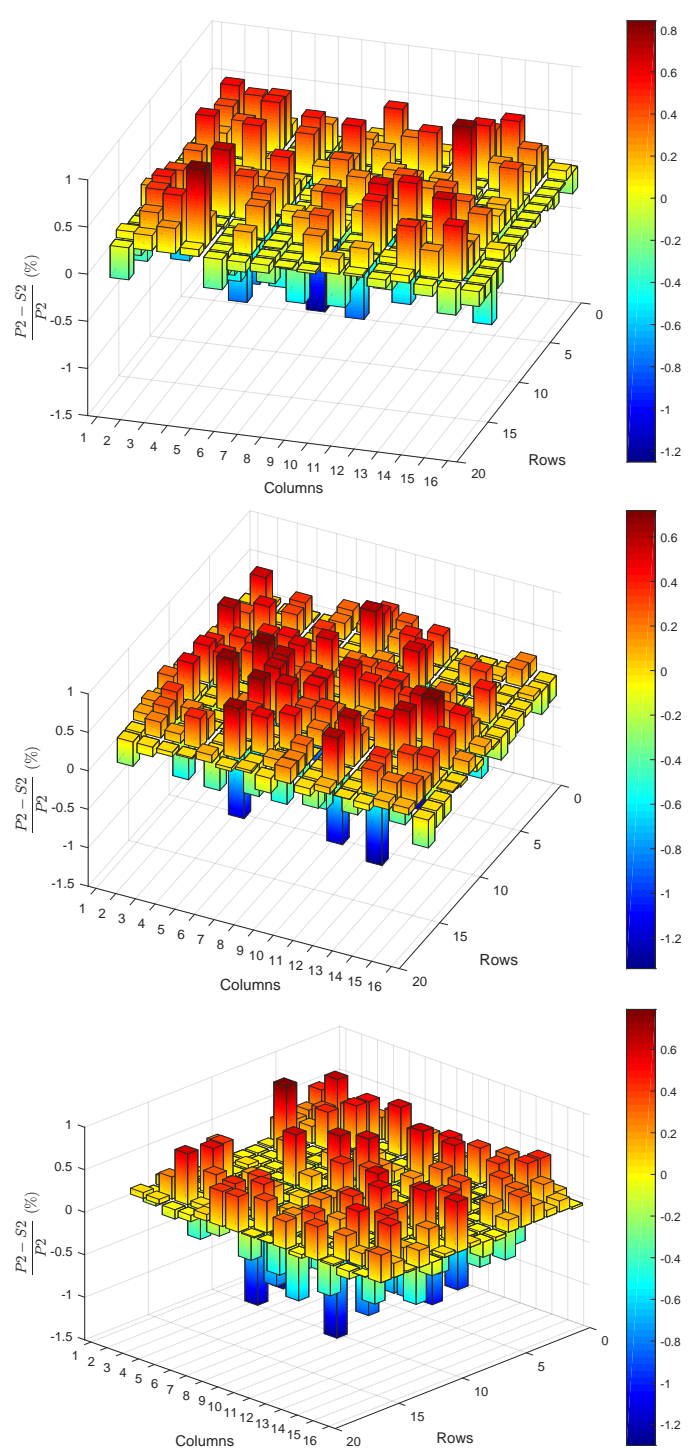


Fig. 13. Pin Power Comparison for Westinghouse 16x16 Assembly with IFBA between PARAGON2 (P2) and SERPENT2 (S2). The top, middle, and bottom figures correspond to the burnups of 0, 10, and 70 GWD/MTU.

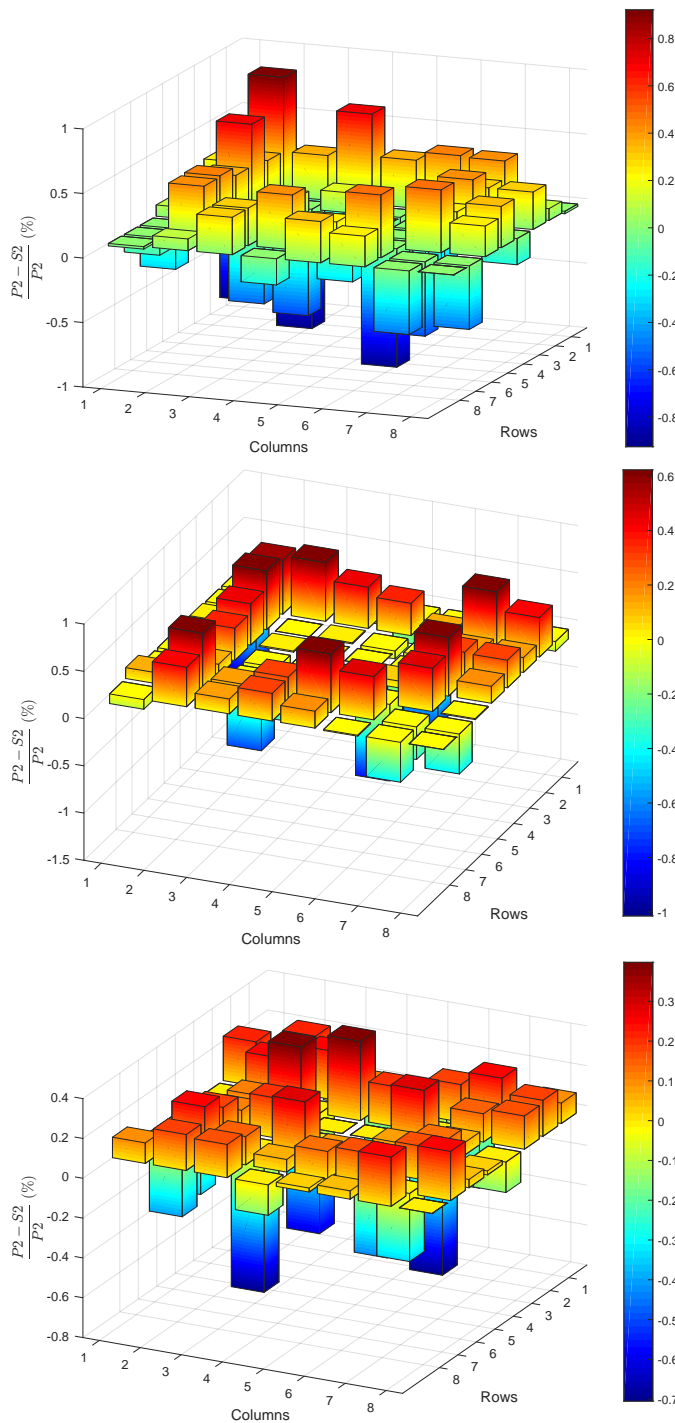


Fig. 14. Pin Power Comparison for CE 16x16 Assembly with IFBA between PARAGON2 (P2) and SERPENT2 (S2). The top, middle, and bottom figures correspond to the burnups of 0, 10, and 70 GWD/MTU.

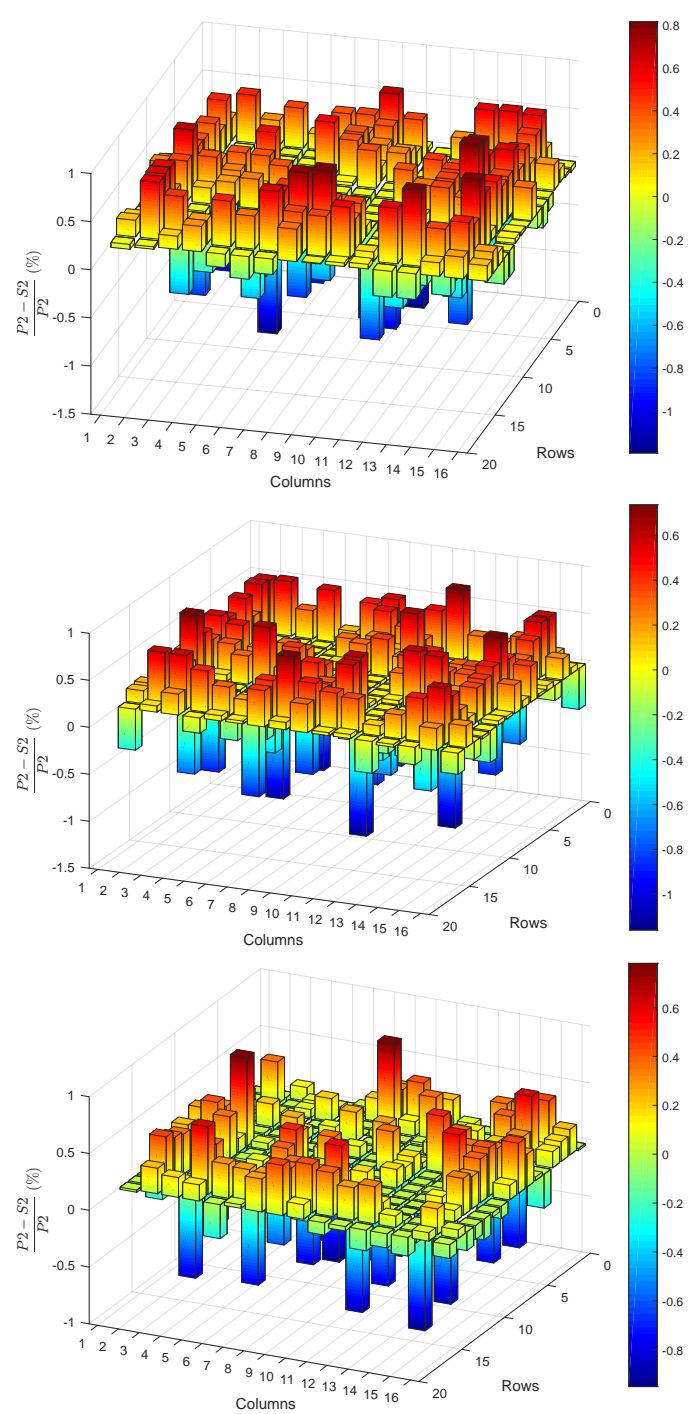


Fig. 15. Pin Power Comparison for CE 16x16 Assembly with ATF between PARAGON2 (P2) and SERPENT2 (S2). The top, middle, and bottom figures correspond to the burnups of 0, 10, and 70 GWD/MTU.

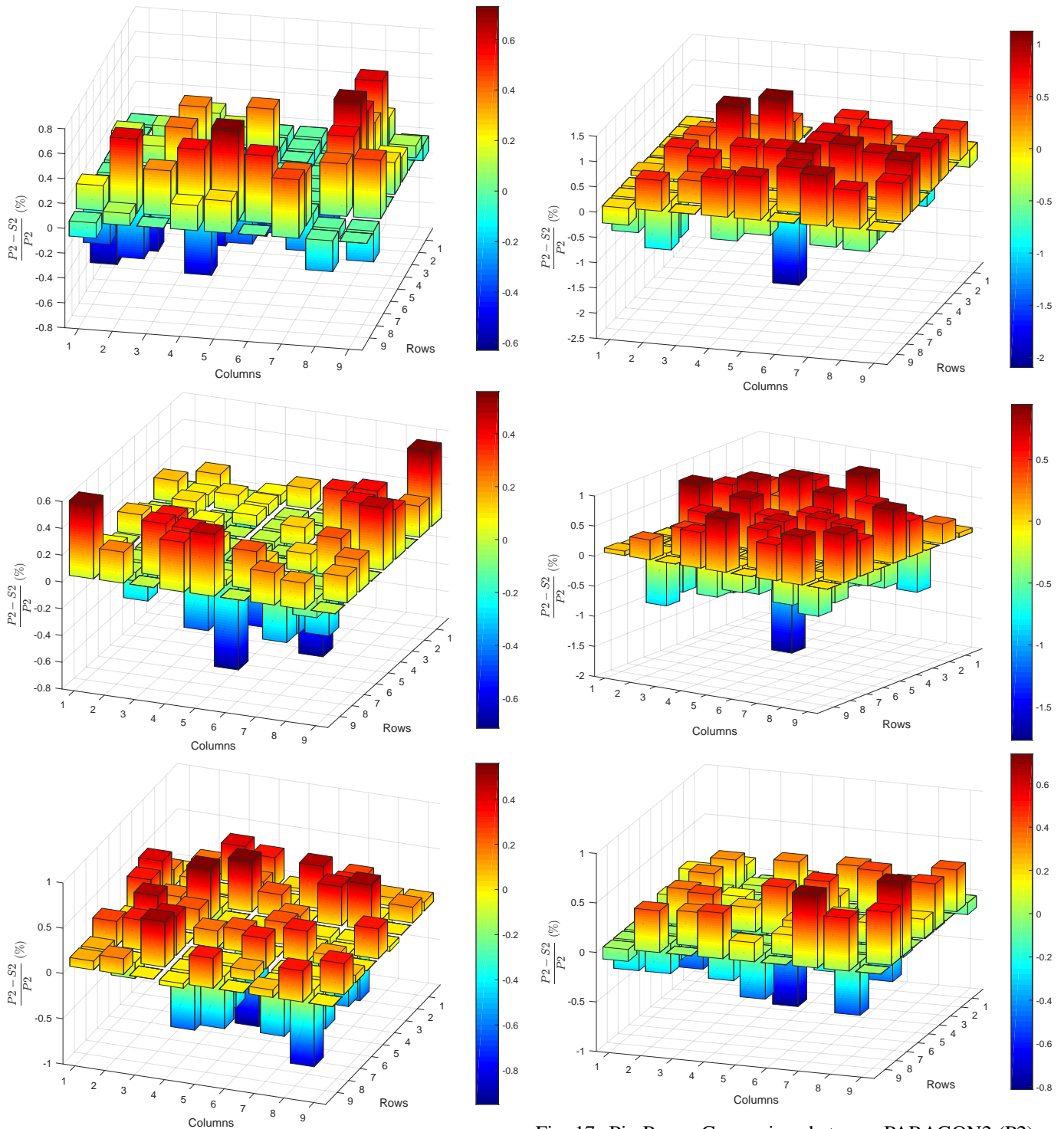


Fig. 16. Pin Power Comparison between PARAGON2 (P2) and SERPENT2 (S2) for 17x17 Assembly with IFBA and WABA. The top, middle, and bottom figures correspond to the burnups of 0, 10, and 70 GWD/MTU.

Fig. 17. Pin Power Comparison between PARAGON2 (P2) and SERPENT2 (S2) for 17x17 MOX Assembly. The top, middle, and bottom figures correspond to the burnups of 0, 10, and 70 GWD/MTU.

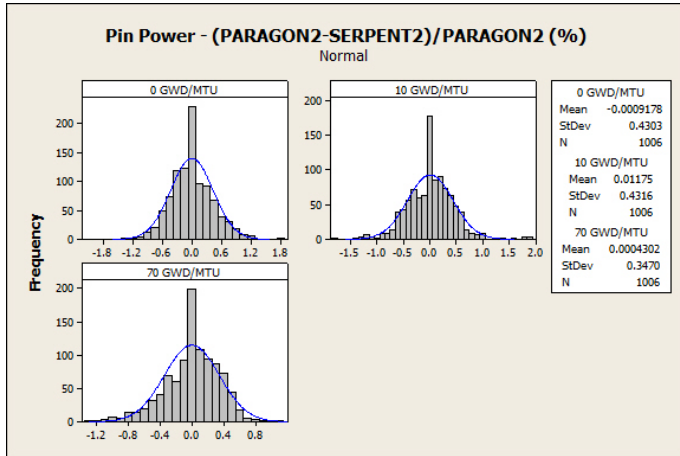


Fig. 18. Histogram of the pin power differences.

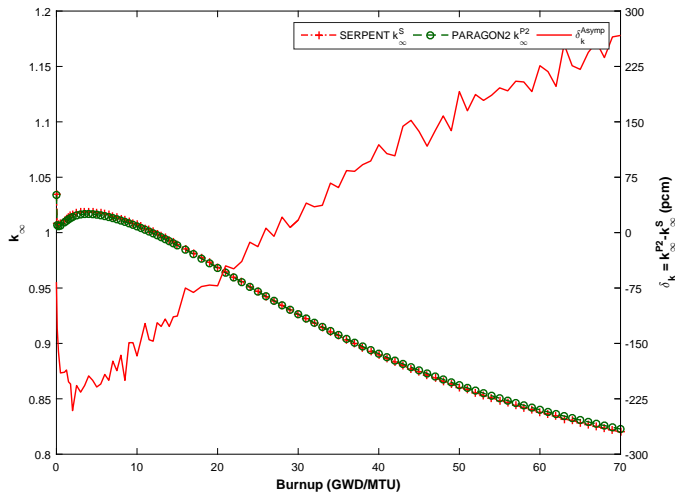


Fig. 19. 17x17 IFBA and WABA Assembly with 50% void - Reactivity Comparison

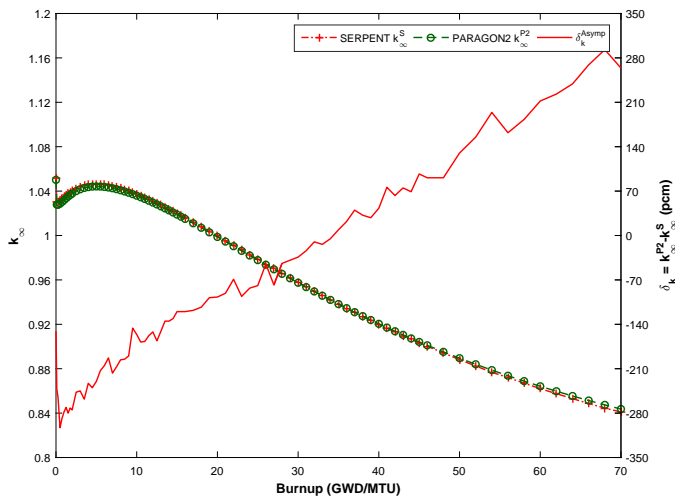


Fig. 20. 17x17 IFBA and WABA Assembly with 50% void - Reactivity Comparison